Geo-Energy Research
Vol. 5, No. 1, p. 39-52, 2021

Original article

Evaluation of asphaltene adsorption on minerals of dolomite and sandstone formations in two and three-phase systems

Mohammad-Reza Mohammadi[1]*, Hamid Bahmaninia[1], Sajjad Ansari[1], Abdolhossein Hemmati-Sarapardeh[1,3]*, Saeid Norouzi-Apourvari[1], Mahin Schaffie[1], Mohammad Ranjbar[1,2]

[1]*Department of Petroleum Engineering, Shahid Bahonar University of Kerman, Kerman, Iran*
[2]*Department of Mining Engineering, Shahid Bahonar University of Kerman, Kerman, Iran*
[3]*College of Construction Engineering, Jilin University, Changchun 130012, P. R. China*

Keywords:
Asphaltene adsorption
dolomite
quartz
magnetite
reservoir rock minerals
static and dynamic adsorption

Cited as:
Mohammadi, M. R., Bahmaninia, H., Ansari, S., Hemmati-Sarapardeh, A., Norouzi-Apourvari, S., Schaffie, M., Ranjbar, M. Evaluation of asphaltene adsorption on minerals of dolomite and sandstone formations in two and three-phase systems. Advances in Geo-Energy Research, 2021, 5(1): 39-52, doi: 10.46690/ager.2021.01.05

Abstract:
Asphaltene adsorption on reservoir rock minerals causes wettability alteration and pore plugging which subsequently reduces crude oil production. Also, it has a negative effect on the efficiency of production and enhanced oil recovery operations. In this study, the adsorption of extracted asphaltenes of two samples of Iranian oil fields on dolomite, quartz, and magnetite was investigated in two- and three-phase systems in both static and dynamic flow modes. Mineral adsorbents were analyzed by Brunauer-Emmett-Teller and X-ray fluorescence methods. Also, several laboratory tests including elemental analysis, field emission scanning electron microscopy, and Fourier transform infrared spectroscopy were carried out to characterize asphaltenes. The results showed that in addition to the effect of known parameters such as asphaltenes concentration and specific surface area of the solid phase, the water phase also affects the amount of asphaltenes adsorption. The adsorption amount of asphaltenes increases with increasing the specific surface area of adsorbent (decreasing particle size) and increasing the initial concentration of asphaltenes, and decreases with the addition of water to the two-phase system. The static adsorption amount of asphaltenes in a two-phase system can be up to 90% higher than the adsorption amount in a three-phase system. Doubling the fluid flow rate in dynamic adsorption significantly (by about 20%) reduces the asphaltenes adsorption, which could be a sign of physical adsorption of asphaltenes on adsorbents. The structure and elemental composition of asphaltenes also have a significant effect on asphaltenes adsorption. The asphaltene sample, which had a more aromatic nature and high nitrogen content, had higher adsorption on reservoir rock minerals. Finally, fitting the adsorption equilibrium models with experimental data reveals that the adsorption isotherm model depends on the type and particle size of the adsorbents and the concentration and type of asphaltenes.

1. Introduction

Asphaltene is the most polar, largest, and heaviest colloidal component of crude oil (Adams, 2014). Precipitation of colloidal components of crude oil, especially asphaltenes, occurs as a result of the system going out of steady-state conditions due to physical changes (pressure, temperature, and flow rate) or change in oil composition due to injection in enhanced oil recovery (EOR) operations. Due to the polarity of asphaltene and having different functional groups, asphaltene can be adsorbed on solid surfaces and change the surface properties of the reservoir rock and its phase and flow behavior. Asphaltene adsorption and deposition can negatively affect production efficiency in production and EOR operations (Piro et al., 1996; Adams, 2014). Resins of crude oil play a direct and essential role in the stability of asphaltenes and the prevention of asphaltenes precipitation (Akbarzadeh et al., 2007; Yarranton et al., 2007). In the stable colloidal state, asphaltene colloidal particles are surrounded by resin molecules. The presence of a layer of resins around the asphaltene colloidal particles creates a suitable repulsive force

Yandy Scientific Press

*Corresponding author.
E-mail address: mohammmadi.mrm@gmail.com (M. R. Mohammadi); hamidbahmaninia@yahoo.com (H. Bahmaninia); sajjad.a1994@gmail.com (S. Ansari); hemmati@uk.ac.ir (A. Hemmati-Sarapardeh); norouzi@uk.ac.ir (S. Norouzi-Apourvari); m.schaffie@uk.ac.ir (M. Schaffie); m.ranjbar@uk.ac.ir (M. Ranjbar).

Received January 3, 2021; revised January 21, 2021; accepted January 22, 2021; available online January 26, 2021.

for the asphaltene to be stabilized in the crude oil (Priyanto et al., 2001; Mousavi-Dehghani et al., 2004; Fakher et al., 2019). Also, wax content can shift the asphaltene onset point of precipitation and decrease the asphaltene deposition rate (Joonaki et al., 2020). The asphaltene nano-aggregates can flocculate to form larger particles that can flow through a porous media or adsorb on the rock surface (Wang et al., 2016; Hassanpouryouzband et al., 2017). Adsorption of asphaltene on the surface of reservoir rock minerals is one of the main causes of formation damage, which reduces the permeability of the reservoir rock and gradually changes the surface properties such as wettability alteration (Garrouch and Al-Ruhaimani, 2005; Sim et al., 2005). Asphaltenes extracted from crude oils of various origins are different in the heteroatoms content, amount of aromatic compounds, alkyl side chain length, molecular weight, and aggregation behavior in toluene-normal alkane mixtures (Calemma et al., 1995; Hemmati-Sarapardeh et al., 2020). The nature of asphaltene is one of the most important factors affecting the stability of crude oils and especially the structure and properties of asphaltene composition strongly affect their precipitation problems (Leon et al., 2000). The structure and composition of asphaltenes, especially their aromaticity and polarity, affect the deposition of asphaltenes (Ahooei et al., 2020). Polar groups and heteroatoms, in the molecular structure of asphaltenes and resins, have been introduced as the main factor of adsorption of these colloidal oil components on the surface of charged particles of reservoir rock minerals (Clementz, 1982; Kokal et al., 1995). This is why one of the main mechanisms of the asphaltene inhibitors is occupying the asphaltene active sites and as a result, change the hydrophobicity of asphaltene nano-aggregates. Delay the precipitation and aggregation steps along with interaction of the inhibitors molecules with asphaltenes for the purpose of decreasing the asphaltene particle size before aggregation is some of the other main mechanisms of inhibitors (Joonaki et al., 2017). Preventing the reduction of reservoir pressure is the key factor to prevent asphaltene deposition in reservoirs (Joshi et al., 2001). Also, the use of nanoparticles, especially metal oxide nanoparticles, can prevent precipitation problems by adsorbing asphaltene particles, and it is a new method for this old and important problem of oil reservoirs (Mazloom et al., 2020). On the other hand, the ultrasonic technique, asphaltene inhibitors, asphaltene dispersants, chemical treatment, etc. can be solutions to prevent asphaltene deposition (Gharbi et al., 2017).

The phenomenon of asphaltene adsorption on different surfaces has always been of interest (Acevedo et al., 2000; Marczewski and Szymula, 2002; Alboudwarej et al., 2005; Dudášová et al., 2009; Syunyaev et al., 2009; Adams, 2014; Tsiamis and Taylor, 2017; Taheri-Shakib et al., 2019; Mazloom et al., 2020a, 2020b). González and Middea (1988) examined the adsorption of three samples of asphaltene and resin on calcite and observed that for all cases, the adsorption of asphaltenes was higher than that of resins. The results of this study also revealed that monolayer or multilayer adsorption depends on the type of crude oil (González and Middea, 1988). Marczewski and Szymula (2002) investigated the adsorption of asphaltene from toluene solution on the various adsorbents of quartz, dolomite, calcite, kaolin, Fe_2O_3, and TiO_2. The results of adsorption experiments demonstrated that the asphaltene adsorption model was dependent on concentration (Marczewski and Szymula, 2002). Dudášová et al. (2008) investigated the adsorption of asphaltenes of five various origins onto different inorganic particles. According to the results of this study, the amount of asphaltenes adsorbed on the particle depend on the type of adsorbent, and the amount of asphaltene nitrogen (Dudášová et al., 2008). The asphaltenes removal from heavy crude oil using nickel micro and nanoparticle adsorbents was evaluated by Nassar et al. (2008). It was found that the adsorption capacity of nickel nanoparticles is three times higher than the adsorption capacity of nickel microparticles (Nassar et al., 2008). The roles of water and free gas in the adsorption and even desorption process in different systems can not be ignored (Gou and Xu, 2019; Li et al., 2020). Gonzalez and Taylor (2016) considered the presence of pre-adsorbed water on asphaltene adsorption on quartz sand. Their results illustrated that asphaltene adsorption on quartz is highly affected by surface-adsorbed water, and it decreases linearly with the thickness of adsorbed water film (Gonzalez and Taylor, 2016). Khormali et al. (2018) carried out the adsorption of asphaltene on sandstone and carbonate rock samples and revealed that the adsorption of asphaltene on both rock samples increases with increasing the initial concentration of asphaltene. According to the results of this study, the amount of asphaltene uptake on reservoir rocks is significantly reduced in the presence of asphaltene inhibitors (Khormali et al., 2018). Veisi et al. (2018) investigated the possibility of removing asphaltene from toluene solution using low-cost natural adsorbents, such as bentonite, light expanded clay aggregate (LECA), and perlite, and showed that the efficiency of the operation depends on the type of adsorbent (Veisi et al., 2018). Monjezi et al. (2019) investigated the adsorption of asphaltene on a porous medium containing calcite in a dynamic state in the presence of brine film. They observed that brine creates a mechanical barrier between the surface of calcite and asphaltenes. In the absence of water film, asphaltenes uptake increased 6.5 times (Monjezi et al., 2019). Table 1 summarizes some of the valuable works on the asphaltenes adsorption on minerals.

Despite numerous researches conducted on the effective factors of asphaltene adsorption, a comprehensive theory and model have not been presented in this regard. Therefore, the need to study the adsorption of asphaltenes, with different origins, to achieve a more comprehensive theory is obvious. Therefore, the main purpose of this study, as part of a comprehensive systematic study plan is to pay more attention to the effect of composition of Iranian asphaltenes on their adsorption on the main minerals of the reservoir rocks. In this regard, the adsorption of asphaltenes extracted from two crude oils of Iranian oil fields on three minerals namely dolomite, quartz, and magnetite, is investigated under the conditions of two and three-phase systems. Mineral adsorbents are analyzed by X-ray fluorescence (XRF) and Brunauer-Emmett-Teller (BET) methods. In addition, elemental analysis, field emission scanning electron microscopy (FESEM), and Fourier transform infrared spectroscopy (FTIR) are performed to characterize the

Table 1. Summary of experimental investigations on asphaltene adsorption on minerals.

Mineral adsorbents	Number of asphaltenes	Type of adsorption		Number of phases		References
		Static	Dynamic	2	3	
Kao1inite, Chlorite, Illite, Berea Sandstone	3	*	-	*	*	(Collins and Melrose, 1983)
Calcite, Dolomite, Alumina, Kaolin, Illite, Chlorite, Dickite, Thuringite	1	*	-	*	-	(Dubey and Waxman, 1991)
Kaolin, Smectite, Fluorite, Hematite, Calcite, Quartz, Feldspar	2	*	-	*	-	(González and Moreira, 1994)
Quartz, Kaolinite, Bentonite, Illite, montmorillonite	1	*	-	*	-	(Pernyeszi et al., 1998)
Dolomite, Quartz, Calcite, Kaolin, TiO_2, Fe_2O_3	1	*	-	*	-	(Marczewski and Szymula, 2002)
$BaSO_4$, FeS, Fe_3O_4, $CaCO_3$, TiO_2, SiO_2, Kaolin	5	*	-	*	-	(Dudášová et al., 2008)
Mica, Dolomite, Quartz	1	*	-	*	-	(Syunyaev et al., 2009)
Hematite, Smectite, Kaolin, Fluorite	1	*	-	*	-	(Mohammadi et al., 2014)
Silica sand	1	-	*	*	-	(Nassar et al., 2015)
Silica	1	*	-	*	*	(Hu et al., 2018)

asphaltenes. Afterwards, the effect of asphaltene type and concentration is investigated on their adsorption on three different minerals with two different sizes. In addition, the presence of water in the liquid phase on asphaltene adsorption is studied in static flow condition. Besides, the effect of flow rate on the adsorption process is evaluated in dynamic condition. Finally, adsorption models such as Freundlich, Temkin, Langmuir, and Dubinin-Radushkevich are used to describe the adsorption processes.

2. Materials and methods

2.1 Materials

In this work, relatively pure dolomite, quartz, and magnetite in two different sizes (micro 1 and micro 2) were used as adsorbents. The results of XRF spectrometry are reported in Table 2. Table 3 presents the specific surface areas (BET method) and other specifications of the adsorbents' samples. Adsorbents pores are between 2 and 50 nm and can be classified into mesopores categories (Zdravkov et al., 2007).

Persian Gulf water was used for 3-phase adsorption experiments in this study. The main ions of this water in the total dissolved solids of about 41 g/L, including Na^+, K^+, Ca^{2+} Mg^{2+}, Cl^-, SO_4^{2-}, HCO_3^{2-} with a pH of (7.9) which have been reported elsewhere (Dehaghani and Daneshfar, 2019).

Table 2. Results of XRF analysis of quartz, dolomite and magnetite.

Contents (wt%)	Quartz	Dolomite	Magnetite
SiO_2	97.52	1.13	2.82
Al_2O_3	0.13	0.04	0.29
BaO	<0.01	0.01	<0.01
CaO	0.23	36.02	2.35
Fet*	1.94	6.54	54.31
K_2O	0.01	0.01	<0.01
MgO	0.04	12.47	9.47
MnO	0.01	0.62	0.05
Na_2O	0.05	0.09	0.06
P	0.04	0.03	0.24
S	0.14	<0.05	1.91
TiO_2	0.01	<0.01	0.01
Cr_2O_3	<0.01	<0.01	<0.01
Cu	<0.01	<0.01	<0.01
Pb	<0.01	<0.01	<0.01
Zn	<0.01	<0.01	<0.01
LOI**	-0.12	43.04	6.89

Note: *: total Fe, **: loss on ignition

Table 3. Specification of mineral adsorbents.

Mineral adsorbent	Specific surface area (BET) (m^2/g)	Pore volume (cm^3/g)	Average pore diameter (nm)	Particle size (μm)
Micro-quartz 1	0.6349	0.0023	14.72	80-400
Micro-quartz 2	1.75	0.009	20.56	30-70
Micro-dolomite 1	1.31	0.0071	21.77	80-400
Micro-dolomite 2	2.46	0.0143	23.28	30-70
Micro-magnetite 1	0.3127	0.0021	26.73	80-400
Micro-magnetite 2	1.97	0.0097	19.67	30-70

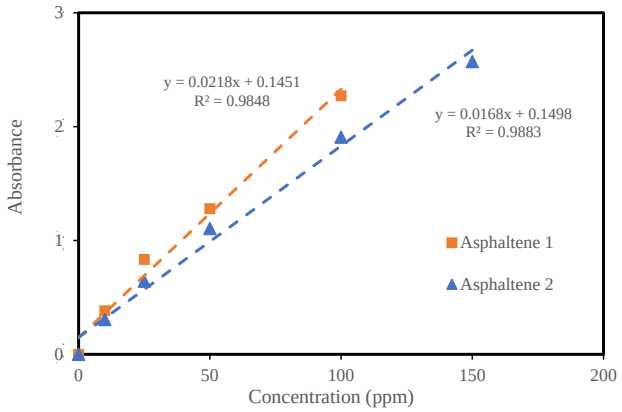

Fig. 1. Calibration curve of asphaltene samples.

2.2 Methods

2.2.1 Characterization of asphaltenes

In this study, the adsorption of two asphaltene samples extracted from crude oils of Iranian oil fields with different origins on the most important reservoir rock minerals was investigated. ASTM standard (D2007-80) (Wang and Buckley, 2006) was applied to extract asphaltenes from crude oils. Elemental analysis was utilized to determine the elements present in asphaltene samples. The surface properties and morphology of asphaltenes were investigated by applying FESEM analysis. FTIR analysis was considered to identify major functional groups in asphaltene samples.

2.2.2 Preparation of asphaltene/toluene solutions

To prepare different concentrations of asphaltenes/toluene solutions, the dilution method was used and samples with different concentrations (0, 100, 200, 500, 1000 ppm) were prepared. First, the absorption of several specific concentrations of asphaltenes/toluene solutions was measured with UV-Vis spectrophotometer at a constant wavelength of 410 nm. This wavelength was regarded as suitable and within the instrument absorbance threshold as it presented appropriate sensitivity to evaluate asphaltene concentrations (Alboudwarej et al., 2005; Ezeonyeka et al., 2018). Thus, it eventually led to the creation of calibration curves and equations of the best trend line from the measured points (Fig. 1).

2.2.3 Static adsorption experiments

In the first phase of the experiments of this study, the static adsorption of asphaltenes was studied. In this case, a certain amount of adsorbent was added to a certain volume of asphaltene/toluene solutions, with different concentrations, (mineral: solution ratio of 1:10), and after mixing with 250 rpm at a constant temperature (25 °C) and atmospheric pressure (14.7 psia) utilizing shaker-incubator (Stuart SI 50, England), it was kept and the amount of remaining asphaltene was determined after a specified time (18 hours). It is noteworthy that in the initial static experiments, the adsorption equilibrium time was measured to be 2 hours. Finally, the amount of adsorbed asphaltene was determined using Eq. (1):

$$q = \frac{V(C_0 - C_e)}{Am} \tag{1}$$

where q denotes the amount of asphaltene adsorption (mg asphaltene/m^2 adsorbent particle), C_0 and C_e are the initial asphaltenes concentration and equilibrium concentration after asphaltene adsorption (mg/L), respectively, V stands for the solution volume (L), m is the adsorbent mass (g) and A expresses the specific surface area of adsorbent particles (m^2). The amount of asphaltene removed from the asphaltene/toluene solution was also calculated by applying Eq. (2):

$$\text{Asphaltene removal } (\%) = \frac{C_0 - C_e}{C_0} \times 100 \tag{2}$$

2.2.4 Static adsorption experiments in the 3-phase system

To investigate the effect of water phase on asphaltenes uptake in a three-phase system, Persian Gulf water and asphaltene solution in a ratio of 1:1, were used. Actually, the mass of asphaltenes in the organic solution is the same in the two- and three-phase systems and the only difference is the presence of water in the three-phase system, in the same ratio as the organic solution. Unlike some other papers that first exposed minerals to water and then examined the amount of asphaltene adsorbed on them, in this work, mineral adsorbents were added to the system containing water and asphaltene/toluene solution to study the competitive performance of water and asphaltene in the adsorption process.

2.2.5 Dynamic adsorption experiments

To evaluate the dynamic behavior of asphaltene adsorption on minerals, a continuous flow adsorption test was performed

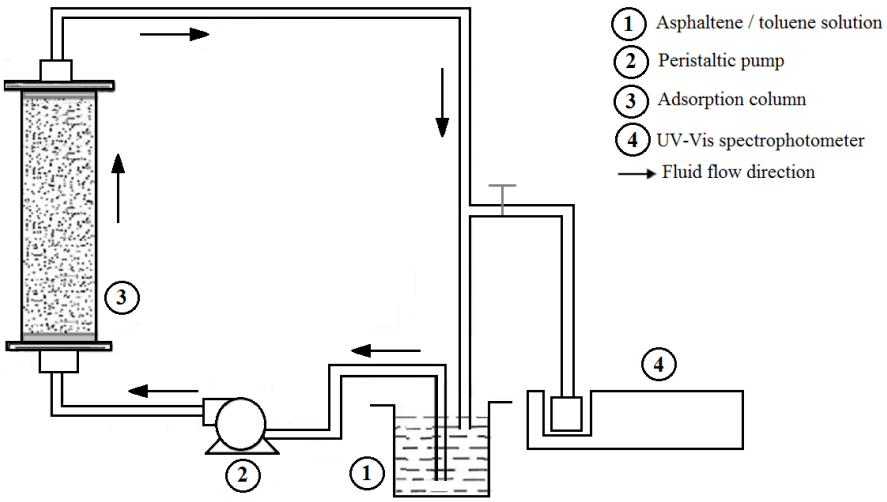

Fig. 2. Schematic of dynamic asphaltenes adsorption tests.

on a fixed-bed polyethylene terephthalate column with a height of 6 cm and an internal diameter of 2 cm. Schematic of equipment used for the dynamic adsorption test is presented in Fig. 2. In this method, asphaltenes solution with a concentration of 100 ppm, with flow rates of 5 and 10 ml/min, is injected into the adsorbent column, from bottom to top. The mineral: solution ratio was again considered 1:10. In this case, the amount of asphaltenes adsorbed is calculated from the outlet solution of the column at certain times.

2.3 Adsorption isotherm models

Langmuir, Temkin, Freundlich, and Dubinin-Radushkevich models were implemented to model the asphaltene adsorption on mineral adsorbents. The non-linear form of these models is presented in the subsequent equations.

$$\text{Langmuir}: q_e = \frac{Q_m k_L C_e}{1 + k_L C_e} \tag{3}$$

$$\text{Freundlich}: q_e = k_F C_e^{\frac{1}{n}} \tag{4}$$

$$\text{Temkin}: q_e = \frac{RT}{b} \ln k_T C_e \tag{5}$$

$$\text{Dubinin-Radushkevich}: q_e = q_s \exp\left(-k_{ads}\varepsilon^2\right) \tag{6}$$

More details about these models can be found in the literature (Langmuir, 1916; Foo and Hameed, 2010; Kecili and Hussain, 2018).

3. Results and discussion

3.1 Characterization of asphaltenes

The results of elemental analysis of asphaltene samples are reported in Table 4. The asphaltenes H/C molar ratio is in the range of other asphaltenes stated in the literature (Zhao and Shaw, 2007; Ezeonyeka et al., 2018).

The results of FESEM analysis of asphaltenes (Fig. 3) show the difference in their surface properties and morphology. The formation of small cavities may be due to the resins of oil that surrounds the asphaltenes in crude oil and are removed during the asphaltenes extraction process (McLean and Kilpatrick, 1997; Friberg et al., 1998; Trejo et al., 2009). Agglomerated asphaltenes are also obvious in the structure of asphaltenes. This agglomeration can be as the result of interactions between components in resins or asphaltenes that contain polar functional groups (McLean and Kilpatrick, 1997).

Table 4. Elemental analysis of asphaltene samples.

	C, %	N, %	S, %	O, %	H, %	Molar ratio H/C
Asphaltene 1	82.58	1.47	3.07	4.53	8.35	1.204
Asphaltene 2	81.56	1.13	2.05	6.46	8.8	1.285

The FTIR spectra of the asphaltenes are presented in Fig. 4. The normalization process was accomplished on the basis of asymmetrical stretching of the C-H bond in CH_2 that was observed in both spectra at 2,923 cm^{-1}. Also, major identified peaks and the related functional groups are listed in Table 5.

To provide a better insight into the behavior of asphaltene samples and justify the reason for the difference in their adsorption, different indexes that express the structural properties of asphaltenes can be defined based on the area under the peaks in FTIR analysis. In order to compare asphaltenes, aromatic index (indicating the presence of all aromatic compounds in the sample), aliphatic index (indicating the presence of all aliphatic compounds in the sample), and sulphoxide index (indicating the frequency of S=O bonds in the sample) were calculated from the following equations (Lamontagne et al., 2001; Asemani and Rabbani, 2016):

$$\text{Aromatic index}: \frac{A1600}{A724 + A743 + A814} \tag{7}$$

$$\text{Aliphatic index}: \frac{A1460 + A1376}{\sum A} \tag{8}$$

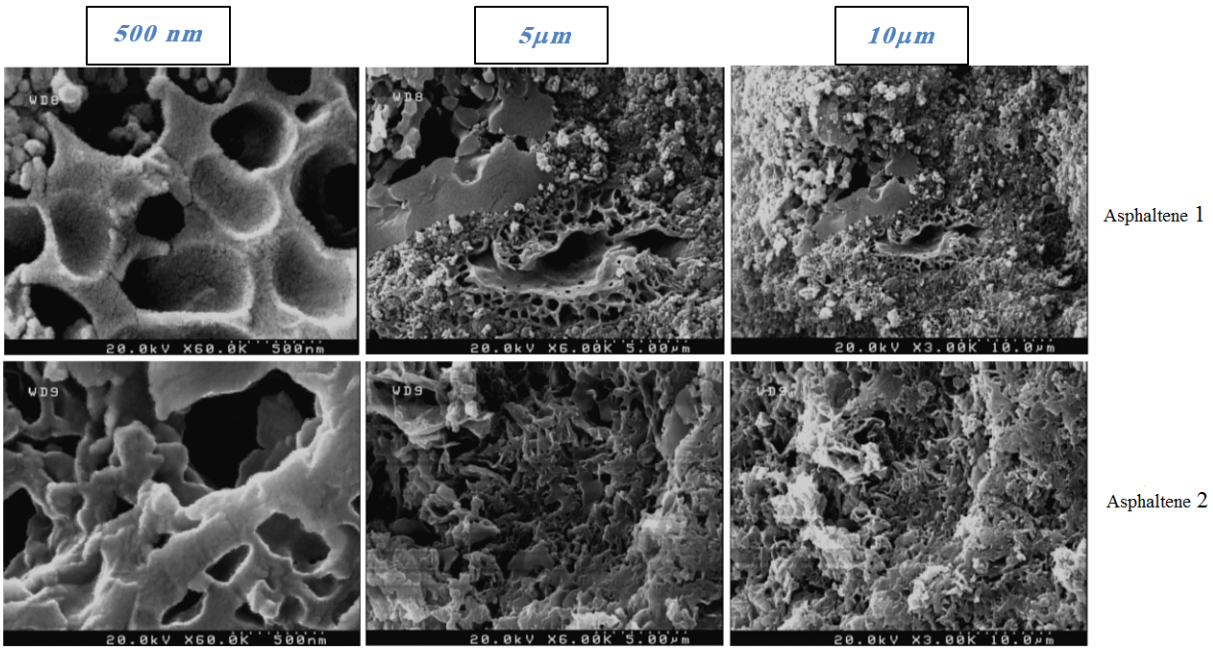

Fig. 3. FESEM images of asphaltene samples surface at different scales.

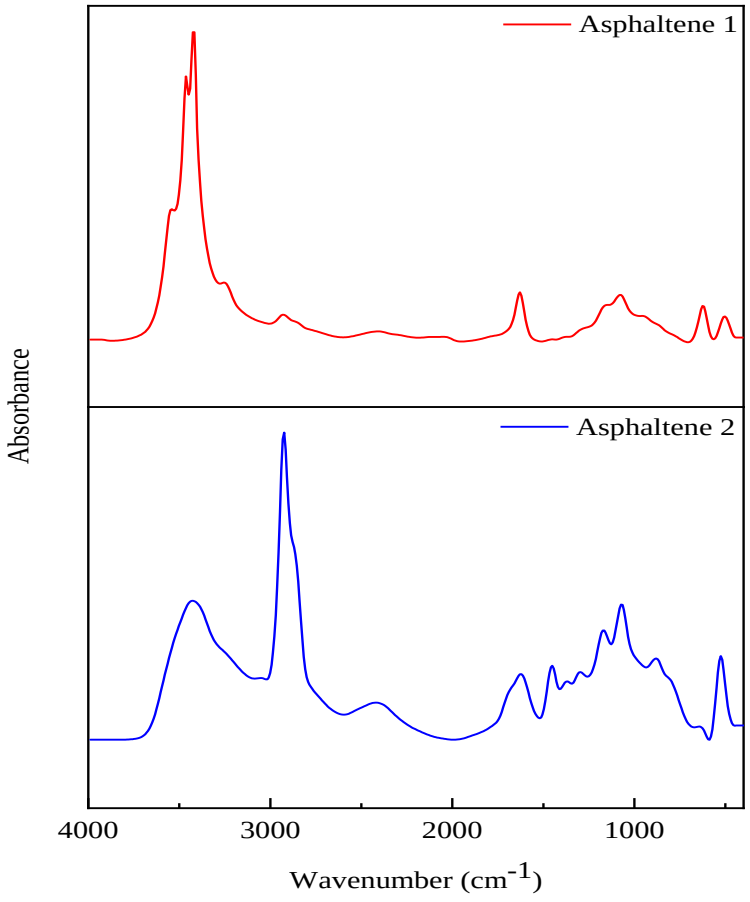

Fig. 4. FTIR spectrum of asphaltene samples.

Table 5. FTIR band assignment of asphaltene samples (Zhao and Shaw, 2007; Franco et al., 2013; Asemani and Rabbani, 2016; Hemmati-Sarapardeh et al., 2018).

Wavenumber, cm^{-1}	Functional group
864, 814, 744, and 724	Out of plane bending of C-H bond in aromatic compounds
1,030	Stretching of S=O bond in sulphoxides
1,159	In plane bending of C-H bond in aromatic compounds
1,315	Bending of C-H bond in CH_3 (wagging and twisting bending) and stretching of C-O bond in carboxylic acid
1,376	Symmetrical bending of C-H bond in CH_3
1460	Symmetrical bending of C-H in CH_2, asymmetrical bending of C-H in CH_3, and asymmetrical stretching of C=C bond in aromatic rings
1,600	Stretching of C=C bond in aromatic rings
2,852	Symmetrical stretching of C-H bond in CH_3 and asymmetrical stretching of C-H bond in CH_2
2,923	Asymmetrical stretching of C-H bond in CH_2
3,430, 3,550	A broad and weak band due to O-H and N-H stretching

Table 6. Structural parameters of asphaltene samples based on FTIR.

	Aromatic Index	Aliphatic Index	Sulphoxide Index
Asphaltene 1	1.35	0.0105	0.1177
Asphaltene 2	0.31	0.0929	0.1294

$$\text{Sulphoxide index: } \frac{A1030}{\sum A} \tag{9}$$

$$\begin{aligned}\sum A =& A2953 + A2923 + A2862 + A1700 + A1600 \\ &+ A1460 + A1376 + A1030 + A864 + A814 \\ &+ A743 + A724\end{aligned} \tag{10}$$

where A denotes the peak area in the absorption spectrum and the subscript number stands for the wave number assigned to the peak. Table 6 compares the values of these indexes for the two asphaltene samples. The results of Table 6 revealed that asphaltene 1 has more aromatic compounds than asphaltene 2, which is consistent with the results of elemental analysis (H/C molar ratio values in Table 4). It is believed that the high aromatic nature of asphaltenes may increase the interaction between asphaltenes and adsorbent, which consequently increases asphaltene uptake (Nassar et al., 2012). The results suggest that the asphaltene 2 molecule has more aliphatic compounds versus asphaltene 1.

3.2 Static adsorption isotherms

Fig. 5 depicts the static adsorption isotherms of asphaltene samples on magnetite, dolomite, and quartz microparticles. The adsorption of asphaltene 1 on minerals is higher than that of asphaltene 2. Various factors such as atomic ratio H/C (aromatic index), molecular mass of asphaltenes, heteroatoms contents, especially nitrogen and sulfur can affect the tendency of asphaltenes to adsorb on adsorbents (Carbognani, 2000; Lopez-Linares et al., 2011; Nassar et al., 2012). Low molecular weight asphaltenes with high nitrogen content and higher aromatic nature are more prone to interact effectively with adsorbents, especially iron-based particles (Nassar et al., 2012). Higher sulfur concentrations increase the adhesion strength of asphaltene to the dolomite surface (Taheri-Shakib et al., 2018). Nitrogen can also be an important element in the adsorption of asphaltenes on dolomite and quartz (Dudášová et al., 2008; Taheri-Shakib et al., 2018). According to the results of Tables 4 and 6, asphaltene 1 has a lower H/C ratio (higher aromatic nature) than asphaltene 2 and it has higher nitrogen and sulfur contents, which can be the reason for more adsorption of asphaltene 1 on minerals. Comparison of Figs. 5(a) and 5(b) reveals that the asphaltenes adsorption (mg asphaltenes/m^2 adsorbent) on micro 1 mineral adsorbents is higher than that of micro 2, which can be due to the higher specific surface area of micro 2 adsorbents than that of micro 1. Adsorption of asphaltene 2 on the adsorbents was lower than asphaltene 1 due to its low aromatic character and low nitrogen content. According to Fig. 5(a), the adsorption amount of asphaltene 1 with 3-14 mg/m^2 is approximately 10-25% higher than the adsorption amount of asphaltene 2 under similar conditions. This increase in adsorption of asphaltene 1 compared to asphaltene 2 on the surface of minerals also can be found in Fig. 5(b). The adsorption capacity of minerals is such that magnetite had the highest adsorption capacity and dolomite had the lowest asphaltenes adsorption capacity. This trend has also been observed in the literature (González and Moreira, 1994; Adams, 2014). Minerals containing iron oxides have different adsorption isotherms than other non-clay minerals and minerals containing clay (González and Moreira, 1994; Adams, 2014). For this reason, magnetite has shown more adsorption capacity. On the other hand, the addition of different iron compounds to asphaltenes has a significant effect on their polarity and increases the tendency to asphaltenes precipitation (Nalwaya et al., 1999). Quartz has polar surfaces containing Si-OH and hydroxyl groups. These polar groups are regarded as active sites for asphaltenes adsorption. Quartz is also deemed slightly acidic, while dolomite has weak Ca-OH base groups. Dolomite and calcite are generally positively charged, which can lead to weaker interactions between the

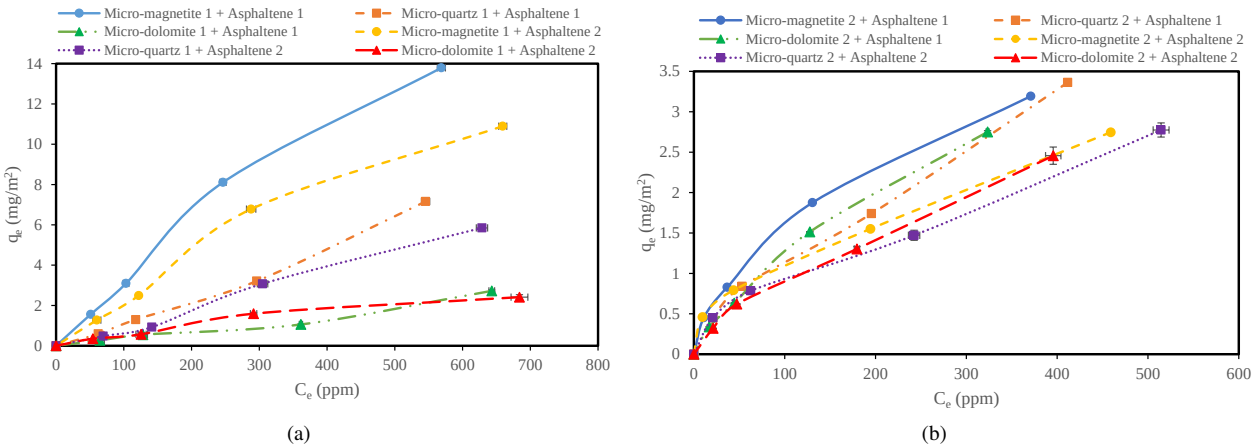

Fig. 5. Static adsorption isotherms of asphaltenes on mineral adsorbents. (a) micro 1; (b) micro 2.

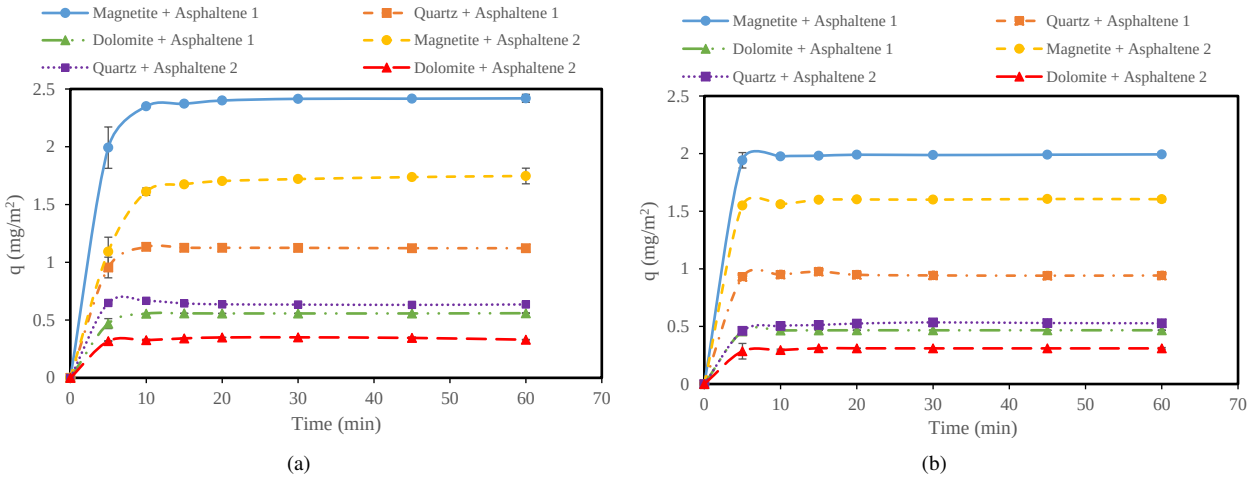

Fig. 6. Adsorption of asphaltenes on micro 1 minerals in the dynamic state for flow rates. (a) 5 ml/min; (b) 10 ml/min.

asphaltenes and calcium hydroxyl functional groups (Adams, 2014). One of the main factors in the adsorption process is the specific surface area of the adsorbent, but the study of different adsorption isotherms shows that increasing the tendency and adsorption capacity of minerals by reducing the particle size is beyond increasing the specific surface area. It can depend on other factors such as the dispersion ability and the inherent interactions of asphaltenes and mineral adsorbents.

3.3 Dynamic adsorption of asphaltenes on minerals

To determine the effect of fluid flow rate on adsorption, dynamic tests were performed using the asphaltenes/toluene solution at a concentration of 100 ppm and flow rates of 5 and 10 ml/min. Fig. 6 displays the dynamic adsorption amount of asphaltenes on micro 1 minerals at different times. The results presented in this figure show that, like the results of static adsorption (Fig. 5), in the dynamic state, the adsorption of asphaltene 1 on minerals is higher than the adsorption of asphaltene 2. Also, the adsorption equilibrium time is very fast and after about 10 minutes, the adsorption process reaches equilibrium.

As shown in Fig. 6, for both asphaltene samples, increasing the fluid flow rate from 5 to 10 ml/min reduces the adsorption of asphaltenes on the adsorbents. For better visual comparison, the uptake of asphaltene 1 on mineral adsorbents is demonstrated in Fig. 7. Based on this figure, with increasing fluid flow rate from 5 to 10 ml/min, the adsorption amount of asphaltene 1 on the surface of micro-magnetite 1 decreases from 2.41 to 1.99 mg/m^2, and for micro-quartz 1 and micro-dolomite 1, asphaltene uptake decreases from 1.12 to 0.94 mg/m^2 and from 0.56 to 0.46 mg/m^2, respectively. This decrease in asphaltene uptake on mineral adsorbents has also occurred with increasing flow rate for asphaltene sample 2. Dynamic adsorption experiments in this paper were such that no new feed was injected into the system, i.e., the input and output of the system were in the same container. This causes that the effect of increasing the input energy to the system with an increasing flow rate to be seen. After performing dynamic adsorption tests, the adsorption reaches equilibrium in a short period of time, but reducing the amount of adsorption, by increasing the fluid flow rate, can be a clear sign for the physical adsorption of asphaltenes on the surface of minerals.

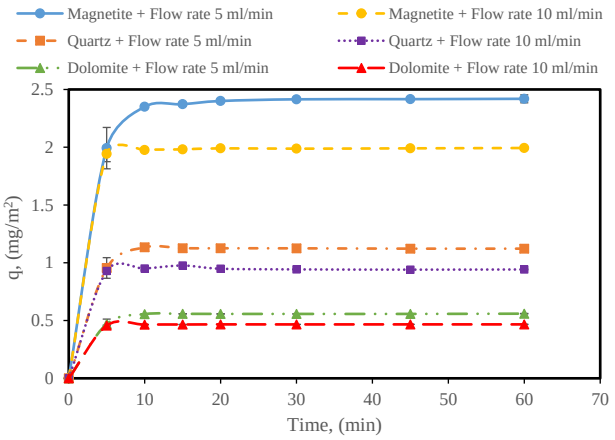

Fig. 7. Comparison of adsorption of asphaltene sample 1 on micro 1 minerals for flow rates of 5 and 10 ml/min.

With the increase of energy entering the system, the filtration created in the openings of the pores are reduced and weaker bonded components are released from the surface of mineral adsorbents. Because physical adsorption, unlike chemical adsorption, is weak and reversible. By investigating the permeability changes before and after asphaltene adsorption, valuable information about dynamic adsorption can be obtained, which is beyond the scope of this article.

Fig. 8 illustrates the percentage of asphaltenes removed from the solution due to adsorption on the surface of various minerals. The results presented in this figure show that by doubling the fluid flow rate, the removal (adsorption) of asphaltenes decreases by about 10 to 20%.

3.4 Asphaltenes adsorption in 3-phase systems

Normally, in crude oil reservoirs, the system consists of three phases (water, crude oil, and reservoir rock). Depending on the type of reservoir wettability, the formation water can have a significant effect on asphaltenes uptake. To investigate the effect of formation water on asphaltene uptake, Persian Gulf water was used. Fig. 9 indicates the adsorption amount of asphaltene 1 and 2 on micro-adsorbents in two and three phase systems. According to the results, it can be said that the asphaltenes adsorption on the surface of mineral adsorbents in the three-phase system and in the presence of water phase for both asphaltene samples 1 and 2, has significantly decreased. According to the results of Fig. 9, the static asphaltenes adsorption in the two-phase system was at least 15% and at most 90% higher than the adsorption amount in the three-phase system. In other words, the highest amount of asphaltenes adsorption occurred in the absence of the water phase, and by adsorption of water on the adsorbents surface, the amount of asphaltenes adsorption decreased. Among different minerals, the reduction of asphaltenes adsorption on the surface of magnetite, which has the highest amount of adsorption in the two-phase system, is more than the other minerals. The interactions of hydrogen bonds are crucial for asphaltene-adsorbents and asphaltenes-asphaltenes interactions, which can be changed remarkably with water. As the adsorbent surfaces are exposed to humidity, the asphaltenes adsorption decreases, because water competes strongly for adsorption sites, but it does not totally prevent the adsorption of asphaltenes (Adams, 2014). Water is one of the strongest fluids to achieve the removal of adsorbed polar hydrocarbons on iron oxides. Iron sequestering agents seem to improve the capability of asphaltenes displacement by water, which may be one of the reasons for the lower adsorption of asphaltene on the magnetite surface in a three-phase system (Carbognani, 2000). From another point of view, the point of zero charge (pzc) of iron oxides is in the range of 8-9 pH, dolomite 6-8 and quartz 1.5-3.7 (Parker, 2001; Pokrovsky et al., 2002; Petrova et al., 2011), and considering that the amount of charges on the surfaces is proportional to (pH_{PZC}-pH) and the ionic strength of the equilibrium solution, the surface charge of magnetite, at pH less than 8 of Persian Gulf water is positive. Therefore, it is expected that the amount of reduction of asphaltenes adsorption on the magnetite surface is higher than the other minerals.

3.5 Adsorption isotherms

The parameters of Langmuir, Temkin, Freundlich, and Dubinin-Radushkevich isotherm models and corresponding coefficient of determination (R^2) and standard deviation (SD) values obtained by fitting these models and experimental data are reported in Tables 7 and 8 for the asphaltenes adsorption onto the surface of micro 1 and micro 2 adsorbents, respectively. Parameters R^2 and SD are defined as follows:

$$R^2 = 1 - \frac{\sum_{i=1}^{N} (q_{e,i} - q_{p,i})^2}{\sum_{i=1}^{N} (q_{p,i} - \overline{q_{e,i}})^2} \tag{11}$$

$$SD = \sqrt{\frac{1}{N-1} \sum_{i=1}^{N} \left(\frac{q_{e,i} - q_{p,i}}{q_{e,i}} \right)^2} \tag{12}$$

where $q_{e,i}$ and $q_{p,i}$ respectively denote the experimental and predicted values of equilibrium adsorption by the isotherm models and N shows the number of data points.

The adsorption of asphaltenes on the surface of micro-magnetite 1 is in a good deal with the Langmuir model, which indicates the adsorption of a single layer of asphaltenes on the adsorbent surface. Freundlich model is in more agreement with the asphaltenes adsorption experimental data onto the surface of micro-magnetite 2, which shows that the adsorption of multilayer nature, with non-uniform distribution, from the adsorption sites. The adsorption data of asphaltene 1 onto the quartz adsorbents fitted well with the Freundlich model and the adsorption of asphaltene 2 onto micro-quartz 1 and 2 are in good consent with the Langmuir and Freundlich models, respectively. The adsorption of asphaltene 1 onto the micro-dolomite 1 and 2 is consistent with the Langmuir and Freundlich models, respectively, and the adsorption of asphaltene 2 on these adsorbents is consistent with the Freundlich and Langmuir models, respectively. In some cases, several models predict the adsorption experimental data well. According to the results, it can be explained that the adsorption isotherm

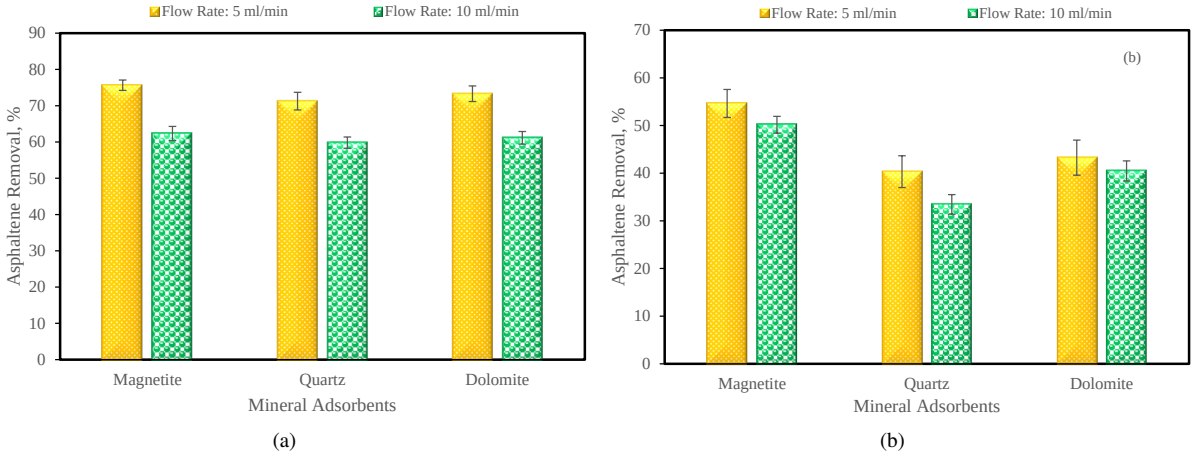

Fig. 8. Effect of flow rate on removal of asphaltenes from solution for asphaltene samples. (a) 1; (b) 2.

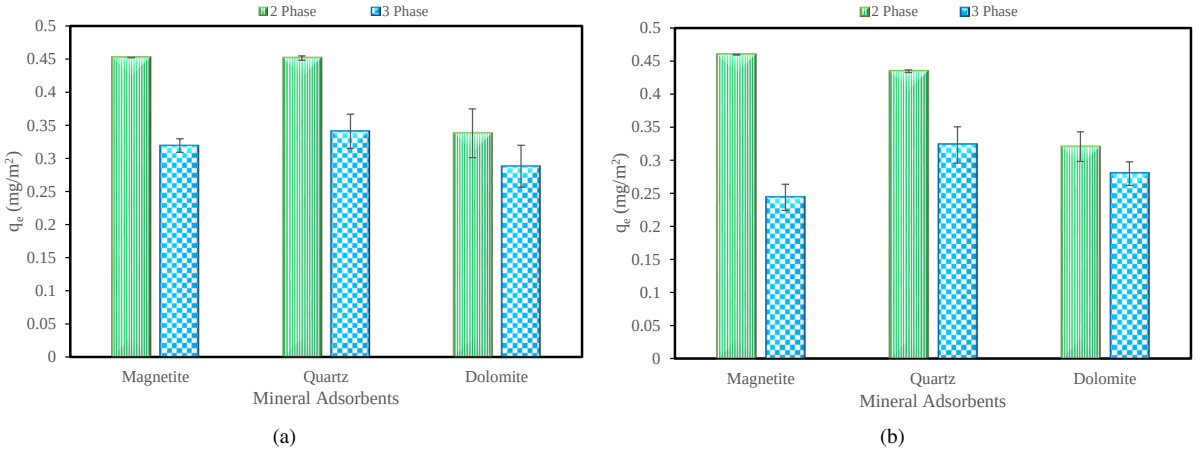

Fig. 9. Comparison of asphaltene (a) 1 (b) 2 adsorption onto the surface of different minerals in two and three phase systems.

model depends on the type and particle size of the adsorbents and the concentration and type of asphaltenes.

The dimensionless separation factor (R_L) is an important property of the Langmuir isotherm, calculated with the following equation.

$$R_L = \frac{1}{1 + K_L C_0} \tag{13}$$

A small amount of R_L indicates more desirable adsorption. Overall, the value of R_L demonstrates that the nature of the adsorption can be linear (R_L = 1), favorable ($0<R_L<1$), unfavorable ($R_L>1$), or irreversible (R_L = 0). R_L values calculated for all adsorption experiments in this study, were obtained between 0 and 1, indicating that the adsorption of asphaltenes on the minerals was appropriate, although the values obtained for micro 2 adsorbents were close to zero and it is more favorable. In the Freundlich model, n is the adsorption intensity constant. Values of $1/n$, in the range of 0.1 to 0.5, indicate strong adsorption, in the range of 0.5 to 1, relatively difficult adsorption, and values of $1/n$, more than 1, indicate weak adsorption. According to the results of Tables 7 and 8, the adsorption of asphaltene samples onto the micro 1 minerals is relatively difficult and even for micro-quartz 1, the adsorption is very poor. Also, according to the results, the adsorption of asphaltenes on micro 2 minerals was relatively stronger than micro 1 minerals. The Dubinin-Radushkevich model has shown the least adaptation in all cases, but the use of this model is important because parameter E in this model represents an insight to check whether adsorption is physical or chemical. If E is less than 8 kJ/mol, the mechanism of adsorption has the nature of physical. If E is between 8 and 16 kJ/mol, the process of adsorption continues through ion exchange. If it is greater than 16 kJ/mol, the mechanism of chemical reaction and particle diffusion dominates the process (Inam et al., 2017). The values of E, presented in Tables 7 and 8, are calculated for the adsorption of asphaltenes on the surface of all adsorbents, less than 8 kJ/mol. Thus, it can be concluded that the asphaltenes adsorption onto the surface of magnetite, dolomite, and quartz minerals has physical nature.

4. Conclusions

In this work, the static and dynamic adsorption of asphaltenes, extracted from two crude oil samples of Iranian oil fields, on the surface of the most important minerals of dolomite and sandstone reservoirs was investigated in two- and

Table 7. Parameters of asphaltenes adsorption isotherm models on micro 1 mineral adsorbents.

Models	Parameter	Micro-magnetite 1		Micro-quartz 1		Micro-dolomite 1	
		AS-1	AS-2	AS-1	AS-2	AS-1	AS-2
Langmuir	K_L (L/mg)	0.00016	0.00015	0.0007	0.00062	0.00055	0.00165
	R_L	0.8607	0.8668	0.9344	0.6143	0.6431	0.3765
	q_{max} (mg/m^2)	168.18	139.01	13.24	10.33	7.85	4.07
	R^2	0.9985	0.9973	0.9955	0.9931	0.9911	0.9628
	SD	0.1105	0.1266	0.3515	0.3994	0.1987	0.1785
Freundlich	K_F	0.0153	0.0094	0.0037	0.0019	0.0069	0.0141
	$1/n$	0.925	0.9239	1.12	1.18	0.9398	0.8543
	R^2	0.9884	0.9831	0.997	0.9876	0.9688	0.9794
	SD	0.2114	0.1206	0.06	0.1257	0.1854	0.156
Temkin	b_T (J/mol)	1526.74	1909.72	1359.74	1572.65	1975.78	1995.66
	K_T (L/mg)	0.0217	0.0188	0.0156	0.0135	0.0158	0.0204
	R^2	0.9658	0.9695	0.8816	0.9258	0.8053	0.9366
	SD	0.4273	0.4116	0.7134	0.868	0.6483	0.5291
Dubinin-Radushkevich	k_{ads}	0.0008	0.0011	0.0014	0.0017	0.0013	0.0008
	E (J/mol)	25	21.32	18.89	17.14	19.61	25
	q_s (mg/m^2)	8.86	7.16	4.14	3.37	1.46	1.58
	R^2	0.7983	0.7975	0.7994	0.7504	0.7369	0.6887
	SD	0.5209	0.5284	0.5151	0.7295	0.5033	0.6087

Table 8. Parameters of asphaltenes adsorption isotherm models on micro 2 mineral adsorbents.

Models	Parameter	Micro-magnetite 2		Micro-quartz 2		Micro-dolomite 2	
		AS-1	AS-2	AS-1	AS-2	AS-1	AS-2
Langmuir	K_L (L/mg)	0.02	0.0376	0.0077	0.0124	0.0074	0.0059
	R_L	0.0476	0.0258	0.1143	0.0743	0.1188	0.1435
	q_{max} (mg/m^2)	2.45	1.7	3.16	2.11	2.96	2.85
	R^2	0.9601	0.9161	0.9862	0.9602	0.9833	0.9961
	SD	0.2394	0.2921	0.1822	0.2278	0.1224	0.1311
Freundlich	K_F	0.2264	0.3232	0.1067	0.14	0.1055	0.1058
	$1/n$	0.564	0.4351	0.6545	0.5481	0.7233	0.6712
	R^2	0.9974	0.9921	0.993	0.9858	0.9974	0.9938
	SD	0.0443	0.0675	0.0746	0.0956	0.0476	0.0692
Temkin	b_T (J/mol)	1622.15	2431.16	1540.78	2095.36	1233.12	1458.12
	K_T (L/mg)	0.1167	0.1706	0.0584	0.0671	0.0664	0.0596
	R^2	0.9359	0.9018	0.89	0.8741	0.9326	0.9178
	SD	0.4083	0.3429	0.4078	0.3606	0.1971	0.3429
Dubinin-Radushkevich	k_{ads}	0.00003	0.00002	0.0001	0.0001	0.00008	0.0001
	E (J/mol)	129.09	158.11	70.71	70.71	79.05	70.71
	q_s (mg/m^2)	1.83	1.52	1.91	1.59	1.56	1.47
	R^2	0.6677	0.6324	0.7063	0.6611	0.7007	0.7582
	SD	0.5923	0.5197	0.5544	0.4955	0.6003	0.7531

three-phase systems. This investigation can lead to a better understanding of the mechanism of asphaltene adsorption on the reservoir rock, and considering the effect of various parameters such as the impact of flow rate and the presence of water can help better management of oil wells and reservoirs. The results of this study show that the composition and structure of asphaltenes, especially aromatic nature, and the amount of heteroatoms, especially nitrogen, have a significant effect on asphaltenes uptake on the surface of the reservoir rock minerals. Asphaltenes adsorption seems to increase with increasing aromatic nature and asphaltenes nitrogen content. In the three-phase system and the presence of water, a significant reduction in asphaltenes adsorption was observed, which can be due to the hydrophilicity of mineral adsorbents in this study. This difference in asphaltenes adsorption in 2 and 3 phase systems indicates the importance of the wettability type of reservoir rock. In dynamic asphaltenes adsorption, with increasing fluid flow rate, the asphaltenes uptake decreased, which could be a sign of physical adsorption of asphaltenes on adsorbents. Due to its specific attractive interaction with the asphaltenes aromatic moieties, magnetite had the highest adsorption capacity, followed by quartz and dolomite. However, the reduction in asphaltene adsorption on the magnetite surface is higher than that of other minerals in the three-phase system due to the higher pH_{PZC} and its positive surface charge in the water. Finally, it can be expressed that the adsorption isotherm model depends on the type and particle size of the adsorbents and the concentration and type of asphaltenes.

Nomenclature

AS = Asphaltene
b_T = Temkin constant [J/mol]
C_e = Equilibrium concentration [mg/L]
C_0 = Initial concentration [mg/L]
E = Energy parameter of Dubinin-Radushkevich isotherm [J/mol]
k_{ads} = Dubinin-Radushkevich constant [mol^2/J^2]
k_f = Freundlich adsorption constant [$mg/g(L/mg)^{1/n}$]
k_L = Langmuir equilibrium constant [L/mg]
k_T = Equilibrium binding constant [L/mg]
q_e = Equilibrium adsorption [mg/m^2]
Q_m = Maximum adsorption amount [mg/m^2]
q_s = Dubinin-Radushkevich model monolayer saturation capacity [mg/m^2]
R^2 = Coefficient of determination
R_L = Separation factor
SD = Standard deviation
T = Temperature [K]
ε = Polanyi potential [J^2/mol^2]

Acknowledgement

This research was supported by the National Iranian South Oil Company (NISOC).

Conflict of interest

The authors declare no competing interest.

References

Acevedo, S., Ranaudo, M. A., García, C., et al. Importance of asphaltene aggregation in solution in determining the adsorption of this sample on mineral surfaces. Colloids and Surfaces A: Physicochemical and Engineering Aspects, 2000, 166(1-3): 145-152.

Adams, J. J. Asphaltene adsorption, a literature review. Energy & Fuels, 2014, 28(5): 2831-2856.

Ahooei, A., Norouzi-Apourvari, S., Hemmati-Sarapardeh, A., et al. Experimental study and modeling of asphaltene deposition on metal surfaces via electrodeposition process: The role of ultrasonic radiation, asphaltene concentration and structure. Journal of Petroleum Science and Engineering, 2020, 195: 107734.

Akbarzadeh, K., Hammami, A., Kharrat, A., et al. Asphaltenes-problematic but rich in potential. Oilfield Review, 2007, 19(2): 22-43.

Alboudwarej, H., Pole, D., Svrcek, W. Y., et al. Adsorption of asphaltenes on metals. Industrial & Engineering Chemistry Research, 2005, 44(15): 5585-5592.

Asemani, M., Rabbani, A. R. Oil-oil correlation by ftir spectroscopy of asphaltene samples. Geosciences Journal, 2016, 20(2): 273-283.

Calemma, V., Iwanski, P., Nali, M., et al. Structural characterization of asphaltenes of different origins. Energy & Fuels, 1995, 9(2): 225-230.

Carbognani, L. Effects of iron compounds on the retention of oil polar hydrocarbons over solid sorbents. Petroleum Science and Technology, 2000, 18(3-4): 335-360.

Clementz, D. M. Alteration of rock properties by adsorption of petroleum heavy ends: Implications for enhanced oil recovery. Paper SPE 10683 Presented at SPE Enhanced Oil Recovery Symposium, Tulsa, Oklahoma, 4-7 April, 1982.

Collins, S. H., Melrose, J. C. Adsorption of asphaltenes and water on reservoir rock minerals. Paper SPE 11800 Presented at SPE Oilfield and Geothermal Chemistry Symposium, Denver, Colorado, 1-3 June, 1983.

Dehaghani, A. H. S., Daneshfar, R. How much would silica nanoparticles enhance the performance of low-salinity water flooding? Petroleum Science, 2019, 16(3): 591-605.

Dubey, S. T., Waxman, M. H. Asphaltene adsorption and desorption from mineral surfaces. SPE Reservoir Engineering, 1991, 6(3): 389-395.

Dudášová, D., Flåten, G. R., Sjöblom, J., et al. Study of asphaltenes adsorption onto different minerals and clays: Part 2. Particle characterization and suspension stability. Colloids and Surfaces A: Physicochemical and Engineering Aspects, 2009, 335(1-3): 62-72.

Dudášová, D., Simon, S., Hemmingsen, P. V., et al. Study of asphaltenes adsorption onto different minerals and clays: Part 1. Experimental adsorption with uv depletion detection. Colloids and Surfaces A: Physicochemical and

Engineering Aspects, 2008, 317(1-3): 1-9.

Ezeonyeka, N. L., Hemmati-Sarapardeh, A., Husein, M. M. Asphaltenes adsorption onto metal oxide nanoparticles: A critical evaluation of measurement techniques. Energy & Fuels, 2018, 32(2): 2213-2223.

Fakher, S., Ahdaya, M., Elturki, M., et al. Critical review of asphaltene properties and factors impacting its stability in crude oil. Journal of Petroleum Exploration and Production Technology, 2020, 10: 1183-1200.

Foo, K. Y., Hameed, B. H. Insights into the modeling of adsorption isotherm systems. Chemical Engineering Journal, 2010, 156(1): 2-10.

Franco, C. A., Montoya, T., Nassar, N. N., et al. Adsorption and subsequent oxidation of colombian asphaltenes onto nickel and/or palladium oxide supported on fumed silica nanoparticles. Energy & Fuels, 2013, 27(12): 7336-7347.

Friberg, S. E., Yang, H., Midttun, Ø., et al. Location of crude oil resin molecules at an interface-model system. Colloids and Surfaces A: Physicochemical and Engineering Aspects, 1998, 136(1-2): 43-49.

Garrouch, A. A., Al-Ruhaimani, F. A. Simple models for permeability impairment in reservoir rocks caused by asphaltene deposition. Petroleum Science and Technology, 2005, 23(7-8): 811-826.

Gharbi, K., Benyounes, K., Khodja, M. Removal and prevention of asphaltene deposition during oil production: A literature review. Journal of Petroleum Science and Engineering, 2017, 158: 351-360.

González, G., Middea, A. The properties of the calcite-solution interface in the presence of adsorbed resins or asphaltenes. Colloids and Surfaces, 1988, 33: 217-229.

González, G., Moreira, M. B. C. Chapter 9 the adsorption of asphaltenes and resins on various minerals. Developments in Petroleum Science, 1994, 40: 207-231.

Gonzalez, V., Taylor, S. E. Asphaltene adsorption on quartz sand in the presence of pre-adsorbed water. Journal of Colloid and Interface Science, 2016, 480: 137-145.

Gou, Q., Xu, S. Quantitative evaluation of free gas and adsorbed gas content of Wufeng-Longmaxi shales in the Jiaoshiba area, Sichuan Basin, China. Advances in Geo-Energy Research, 2019, 3(3): 258-267.

Hassanpouryouzband, A., Joonaki, E., Taghikhani, V., et al. New two-dimensional particle-scale model to simulate asphaltene deposition in wellbores and pipelines. Energy & Fuels, 2017, 32(3): 2661-2672.

Hemmati-Sarapardeh, A., Ameli, F., Ahmadi, M., et al. Effect of asphaltene structure on its aggregation behavior in toluene-normal alkane mixtures. Journal of Molecular Structure, 2020, 1220: 128605.

Hemmati-Sarapardeh, A., Dabir, B., Ahmadi, M., et al. Toward mechanistic understanding of asphaltene aggregation behavior in toluene: The roles of asphaltene structure, aging time, temperature, and ultrasonic radiation. Journal of Molecular Liquids, 2018, 264: 410-424.

Hu, X., Yutkin, M. P., Hassan, S., et al. Asphaltene adsorption from toluene onto silica through thin water layers. Langmuir, 2018, 35(2): 428-434.

Inam, E., Etim, U. J., Akpabio, E. G., et al. Process optimization for the application of carbon from plantain peels in dye abstraction. Journal of Taibah University for Science, 2017, 11(1): 173-185.

Joonaki, E., Burgass, R., Hassanpouryouzband, A., et al. Comparison of experimental techniques for evaluation of chemistries against asphaltene aggregation and deposition: New application of high-pressure and high-temperature quartz crystal microbalance. Energy & Fuels, 2017, 32(3): 2712-2721.

Joonaki, E., Hassanpouryouzband, A., Burgass, R., et al. Effects of waxes and the related chemicals on asphaltene aggregation and deposition phenomena: Experimental and modeling studies. ACS Omega, 2020, 5(13): 7124-7134.

Joshi, N. B., Mullins, O. C., Jamaluddin, A., et al. Asphaltene precipitation from live crude oil. Energy & Fuels, 2001, 15(4): 979-986.

Kecili, R., Hussain, C. M. Mechanism of adsorption on nanomaterials. Nanomaterials in Chromatography, 2018, 2018: 89-115.

Khormali, A., Sharifov, A. R., Torba, D. I. Experimental and modeling study of asphaltene adsorption onto the reservoir rocks. Petroleum Science and Technology, 2018, 36(18): 1482-1489.

Kokal, S., Tang, T., Schramm, L., et al. Electrokinetic and adsorption properties of asphaltenes. Colloids and Surfaces A: Physicochemical and Engineering Aspects, 1995, 94(2-3): 253-265.

Lamontagne, J., Dumas, P., Mouillet, V., et al. Comparison by fourier transform infrared (ftir) spectroscopy of different ageing techniques: Application to road bitumens. Fuel, 2001, 80(4): 483-488.

Langmuir, I. The constitution and fundamental properties of solids and liquids. Part i. Solids. Journal of the American Chemical Society, 1916, 38(11): 2221-2295.

Leon, O., Rogel, E., Espidel, J., et al. Asphaltenes: Structural characterization, self-association, and stability behavior. Energy & Fuels, 2000, 14(1): 6-10.

Li, A., Han, W., Fang, Q., et al. Experimental investigation of methane adsorption and desorption in water-bearing shale. Capillarity, 2020, 3(3): 45-55.

Lopez-Linares, F., Carbognani, L., Hassan, A., et al. Adsorption of athabasca vacuum residues and their visbroken products over macroporous solids: Influence of their molecular characteristics. Energy & Fuels, 2011, 25(9): 4049-4054.

Marczewski, A. W., Szymula, M. Adsorption of asphaltenes from toluene on mineral surface. Colloids and Surfaces A: Physicochemical and Engineering Aspects, 2002, 208(1-3): 259-266.

Mazloom, M. S., Hemmati-Sarapardeh, A., Husein, M. M., et al. Application of nanoparticles for asphaltenes adsorption and oxidation: A critical review of challenges and recent progress. Fuel, 2020a, 279: 117763.

Mazloom, M. S., Rezaei, F., Hemmati-Sarapardeh, A., et al. Artificial intelligence based methods for asphaltenes adsorption by nanocomposites: Application of group

method of data handling, least squares support vector machine, and artificial neural networks. Nanomaterials, 2020b, 10(5): 890.

McLean, J. D., Kilpatrick, P. K. Comparison of precipitation and extrography in the fractionation of crude oil residua. Energy & Fuels, 1997, 11(3): 570-585.

Mohammadi, M., Khamehchi, E., Sedighi, M. The prediction of asphaltene adsorption isotherm constants on mineral surfaces. Petroleum Science and Technology, 2014, 32(7): 870-877.

Monjezi, R., Ghotbi, C., Behbahani, T. J., et al. Experimental investigation of dynamic asphaltene adsorption on calcite packs: The impact of single and mixed-salt brine films. The Canadian Journal of Chemical Engineering, 2019, 97(7): 2028-2038.

Mousavi-Dehghani, S. A., Riazi, M. R., Vafaie-Sefti, M., et al. An analysis of methods for determination of onsets of asphaltene phase separations. Journal of Petroleum Science and Engineering, 2004, 42(2-4): 145-156.

Nalwaya, V., Tantayakom, V., Piumsomboon, P., et al. Studies on asphaltenes through analysis of polar fractions. Industrial & Engineering Chemistry Research, 1999, 38(3): 964-972.

Nassar, N. N., Al-Jabari, M. E., Husein, M. M. Removal of asphaltenes from heavy oil by nickel nano and micro particle adsorbents. Paper Presented at Proceedings of the IASTED International Conference, Crete, Greece, 29 September-1 October, 2008.

Nassar, N. N., Hassan, A., Carbognani, L., et al. Iron oxide nanoparticles for rapid adsorption and enhanced catalytic oxidation of thermally cracked asphaltenes. Fuel, 2012, 95: 257-262.

Nassar, N. N., Montoya, T., Franco, C. A., et al. A new model for describing the adsorption of asphaltenes on porous media at a high pressure and temperature under flow conditions. Energy & Fuels, 2015, 29(7): 4210-4221.

Parker, G. Encyclopedia of Materials: Science and Technology. Amsterdam, the Netherlands, Elsevier, 2001.

Pernyeszi, T., Patzkó, Á., Berkesi, O., et al. Asphaltene adsorption on clays and crude oil reservoir rocks. Colloids and Surfaces A: Physicochemical and Engineering Aspects, 1998, 137(1-3): 373-384.

Petrova, T. M., Fachikov, L., Hristov, J. The magnetite as adsorbent for some hazardous species from aqueous solutions: A review. International Review of Chemical Engineering, 2011, 3(2): 134-152.

Piro, G., Canonico, L. B., Galbariggi, G., et al. Asphaltene adsorption onto formation rock: An approach to asphaltene formation damage prevention. SPE Production & Facilities, 1996, 11(3): 156-160.

Pokrovsky, O., Schott, J., Mielczarski, J. Surface speciation of dolomite and calcite in aqueous solutions. Encyclopedia of Surface and Colloid Science, 2002, 4: 5081-5095.

Priyanto, S., Mansoori, G. A., Suwono, A. Structure and properties of micelles and micelle coacervates of asphaltene macromolecule. Prepar for Presented at 2001 American Institute of Chemical Engineers Annual Meet, 2001.

Sim, S. S., Okatsu, K., Takabayashi, K., et al. Asphaltene-induced formation damage: Effect of asphaltene particle size and core permeability. Paper SPE 95515 Presented at SPE Annual Technical Conference and Exhibition, Dallas, Texas, 9-12 October, 2005.

Syunyaev, R. Z., Balabin, R. M., Akhatov, I. S., et al. Adsorption of petroleum asphaltenes onto reservoir rock sands studied by near-infrared (nir) spectroscopy. Energy & Fuels, 2009, 23(3): 1230-1236.

Taheri-Shakib, J., Hosseini, S. A., Kazemzadeh, E., et al. Experimental and mathematical model evaluation of asphaltene fractionation based on adsorption in porous media: Dolomite reservoir rock. Fuel, 2019, 245: 570-585.

Taheri-Shakib, J., Rajabi-Kochi, M., Kazemzadeh, E., et al. A comprehensive study of asphaltene fractionation based on adsorption onto calcite, dolomite and sandstone. Journal of Petroleum Science and Engineering, 2018, 171: 863-878.

Trejo, F., Ancheyta, J., Rana, M. S. Structural characterization of asphaltenes obtained from hydroprocessed crude oils by sem and tem. Energy & Fuels, 2009, 23(1): 429-439.

Tsiamis, A., Taylor, S. E. Adsorption behavior of asphaltenes and resins on kaolinite. Energy & Fuels, 2017, 31(10): 10576-10587.

Veisi, S., Sefti, M. V., Mahdi, S. M., et al. Adsorption behavior of petroleum asphaltenes dissolved in toluene by low-cost mineral adsorbents. Journal of Oil, Gas and Petrochemical Technology, 2018, 5(1): 1-24.

Wang, J., Buckley, J. Standard procedure for separating asphaltenes from crude oils. 2006.

Wang, M., Hao, Y., Islam, M. R., et al. Aggregation thermodynamics for asphaltene precipitation. AIChE Journal, 2016, 62(4): 1254-1264.

Yarranton, H. W., Fox, W. A., Svrcek, W. Y. Effect of resins on asphaltene self-association and solubility. The Canadian Journal of Chemical Engineering, 2007, 85(5): 635-642.

Zdravkov, B., Čermák, J., Šefara, M., et al. Pore classification in the characterization of porous materials: A perspective. Open Chemistry, 2007, 5(2): 385-395.

Zhao, B., Shaw, J. M. Composition and size distribution of coherent nanostructures in athabasca bitumen and maya crude oil. Energy & Fuels, 2007, 21(5): 2795-2804.